Am J Physiol Cell Physiol 314: C675–C689, 2018.
First published February 14, 2018; doi:10.1152/ajpcell.00221.2017.

RESEARCH ARTICLE

Highly conserved motifs within the large Sec7 ARF guanine nucleotide exchange factor GBF1 target it to the Golgi and are critical for GBF1 activity

Cristian A. Pocognoni,[1]* Ekaterina G. Viktorova,[2]* John Wright,[1] Justyna M. Meissner,[1] Garrett Sager,[1] Eunjoo Lee,[1] George A. Belov,[2] and Elizabeth Sztul[1]

[1]*Department of Cell, Developmental and Integrative Biology, University of Alabama at Birmingham, Birmingham, Alabama; and* [2]*Department of Veterinary Medicine, Virginia-Maryland Regional College of Veterinary Medicine, University of Maryland, College Park, Maryland*

Submitted 25 September 2017; accepted in final form 9 February 2018

Pocognoni CA, Viktorova EG, Wright J, Meissner JM, Sager G, Lee E, Belov GA, Sztul E. Highly conserved motifs within the large Sec7 ARF guanine nucleotide exchange factor GBF1 target it to the Golgi and are critical for GBF1 activity. *Am J Physiol Cell Physiol* 314: C675–C689, 2018. First published February 14, 2018; doi: 10.1152/ajpcell.00221.2017.—Cellular life requires the activation of the ADP-ribosylation factors (ARFs) by Golgi brefeldin A-resistant factor 1 (GBF1), a guanine nucleotide exchange factor (GEF) with a highly conserved catalytic Sec7 domain (Sec7d). In addition to the Sec7d, GBF1 contains other conserved domains whose functions remain unclear. Here, we focus on HDS2 (homology downstream of Sec7d 2) domain because the L1246R substitution within the HDS2 α-helix 5 of the zebrafish GBF1 ortholog causes vascular hemorrhaging and embryonic lethality (13). To dissect the structure/function relationships within HDS2, we generated six variants, in which the most conserved residues within α-helices 1, 2, 4, and 6 were mutated to alanines. Each HDS2 mutant was assessed in a cell-based "replacement" assay for its ability to support cellular functions normally supported by GBF1, such as maintaining Golgi homeostasis, facilitating COPI recruitment, supporting secretion, and sustaining cellular viability. We show that cells treated with the pharmacological GBF1 inhibitor brefeldin A (BFA) and expressing a BFA-resistant GBF1 variant with alanine substitutions of RDR1168 or LF1266 are compromised in Golgi homeostasis, impaired in ARF activation, unable to sustain secretion, and defective in maintaining cellular viability. To gain insight into the molecular mechanism of this dysfunction, we assessed the ability of each GBF1 mutant to target to Golgi membranes and found that mutations in RDR1168 and LF1266 significantly decrease targeting efficiency. Thus, these residues within α-helix 2 and α-helix 6 of the HDS2 domain in GBF1 are novel regulatory determinants that support GBF1 cellular function by impacting the Golgi-specific membrane association of GBF1.

ARF activation; GBF1; GEF; Golgi; GTPase; protein secretion; Sec7

INTRODUCTION

All eukaryotic life requires secretory membrane traffic. In unicellular organisms, secretory traffic sustains transport of components that support cell growth and interactions with the environment. In multicellular organisms, secretory traffic is required for deposition of the extracellular matrix and cell adhesion, the release of growth factors and nutrients, and the insertion of environment-sensing receptor and signal transducers, i.e., all the processes that integrate the developmental and physiological responses of tissues and organs.

A family of ADP-ribosylation factor (ARFs) GTPases has emerged as key regulators of membrane traffic and secretion (27). Like all GTPases, ARFs cycle between an inactive GDP-bound form found in the cytosol and an active GTP-bound state that is membrane associated. The intrinsic exchange capacity of ARFs is extremely low, and in cells, ARF activation is facilitated by a family of guanine nucleotide exchange factors (GEFs) containing a highly conserved catalytic Sec7 domain (Sec7d). The Sec7d consists of ~200 amino acids arranged in 10 α-helices that form a tightly folded domain that binds the substrate ARF and mediates the GDP/GTP exchange (8, 16, 40, 41). In addition to the Sec7d, all GEFs contain other domains that regulate their membrane association and activity (12). Importantly, although the Sec7 domains alone are capable of catalyzing GDP/GTP exchange on ARF in vitro, Sec7 domains are not functional when expressed in cells because they can't target and associate with membranes (11). Thus, regions within GEFs other than the Sec7d control the cellular functionality of each GEF by providing essential membrane targeting and binding information. Understanding the structure/function relationships within conserved domains other than the Sec7d is key for understanding the mechanisms by which ARF activation is regulated within cells.

Golgi homeostasis and secretion requires ARF activation mediated by the Sec7d-containing Golgi brefeldin A-resistant factor 1 (GBF1). Initial insight into the role of GBF1 in cellular life came from studies in yeast. Gea1p and Gea2p (two closely related orthologs of mammalian GBF1), were shown to be required for secretory traffic, and various temperature-sensitive alleles of GEA1 and GEA2 have defects in endoplasmic reticulum (ER)-Golgi transport (26, 49, 59). Studies in mammalian cells confirmed that GBF1 regulates traffic of cargo proteins between the ER and the Golgi (33, 64). One of the essential functions of GBF1-mediated ARF activation is to support continuous membrane traffic by facilitating the formation of recycling COPI vesicles (18, 23, 28, 73). Because GBF1 is required for ER to Golgi traffic (the first step of the secretory pathway), it represents a critical factor for regulating flux through the entire secretory pathway. GBF1 is a cytoplasmic protein that rapidly cycles on and off the membranes of the

* C. A. Pocognoni and E. G. Viktorovaqual contributed equally to this work.
Address for reprint requests and other correspondence: C. A. Pocognoni, Dept. of Cell, Developmental and Integrative Biology, Univ. of Alabama at Birmingham, Birmingham, AL 35233 (e-mail: cpocogno@uab.edu).

ER-Golgi intermediate compartment (ERGIC) and the *cis*-Golgi (18, 28, 73). GBF1 functions in ARF activation only when associated with the membrane, implying that regulation of GBF1 membrane-binding regulates its cellular function.

The functions of some of the conserved domains within GBF1 have been partially characterized: the central Sec7d catalyzes GDP/GTP exchange on ARF, and mutations within Sec7d such as the E794K substitution result in a GBF1 variant that can associate with membranes, but cannot catalyze ARF activation (23, 25, 63, 72). The NH_2 terminus of GBF1 contains two conserved domains (DCB, dimerization and cyclophilin binding, and HUS, homology upstream of Sec7d). The DCB domain has been shown to regulate the oligomeric state of GBF1 by binding either another DCB or the downstream HUS domain, and specific mutations within the DCB abolish oligomer formation but do not affect GBF1 functionality (9, 51). The NH_2-terminal region appears to be essential for membrane association of GBF1, since the deletion of as little as 37 NH_2-terminal residues prevents efficient Golgi targeting (Ref. 6 and data not shown). GBF1 recruitment to membranes is facilitated by the activated form of the small GTPase Rab1b, and the NH_2-terminal 384 amino acids of GBF1 have been shown to interact with Rab1b (1, 39). Within the COOH-terminal portion, GBF1 contains three homology downstream of the Sec7d (HDS1–3) domains. In addition to the NH_2-terminal domain, HDS1 and HDS2 have been shown to be required for GBF1 targeting to the Golgi since deleting only HDS1, only HDS2, or both together, inhibited GBF1 targeting to Golgi membranes in vivo (11, 21). Recently, we have shown that HDS1 participates in GBF1 recruitment to Golgi membranes by binding specific phosphoinositides (PIPs) (37). Furthermore, recombinant HDS1 alone was shown to bind liposomes containing neutral lipids in vitro (35) and to target to lipid droplets in vivo (11). In addition, the HDS1-HDS2 domains have been implicated in chemotactic response of neutrophils in a mechanism involving binding to plasma membrane-localized PIPs (35). The plasma membrane recruitment of GBF1 observed in this study appears cell specific, since GBF1 is not detected on the plasma membrane in the vast majority of non-neutrophil cells. The function of the COOH-terminal HDS3 is currently unknown, but deletion of HDS3 and the downstream region from the *Drosophila* ortholog *Garz* renders the protein inactive (67). Thus, it appears that multiple domains of GBF1 participate in the spatially and temporally restricted recruitment of GBF1 to membranes and thereby regulate its cellular function.

Recently, a report identified the L1246R mutation within the HDS2 domain of zebrafish GBF1 as causative for vascular dysfunction and hemorrhage in early embryos (13), suggesting that HDS2 plays a key role in regulating GBF1 function. Thus, we focused on defining the structure/function relationships within HDS2 of GBF1 as means to understand the cellular regulation of ARF signaling.

The HDS2 domain contains six α-helices, and the L1246R mutation maps to α-helix 5. To provide insight into the functional information within the other helices within HDS2, we targeted conserved amino acids within α-helices 1, 2, 4, and 6 for alanine substitutions. So-generated GBF1 mutants were subsequently assessed for their ability to support Golgi homeostasis and ARF activation, and we found that substitutions within α-helix 2 or 6 impairs the ability of GBF1 to support both functions. To provide insight into the mechanism causing the defect, we examined the ability of the inactive GBF1 mutants to target to the Golgi. We show that lack of functionality correlates with an inhibition in membrane association without significantly affecting the ability of the GBF1 mutants to activate ARF. Thus, specific amino acids within α-helices 2 and 6 of the HDS2 domain facilitate GBF1 association with membranes and represent part of the cellular mechanism that regulates productive cycles of GBF1 membrane binding. The decrease in the efficiency of GBF1 recruitment had dire consequences for the cell, as cells containing GBF1 constructs with mutations in α-helix 2 or 6 were inhibited in secretion and had reduced viability. Our studies identify a novel function for α-helices 2 and 6 within the HDS2 domain as regulators of GBF1 association with Golgi membranes that critically impact cellular function of GBF1.

EXPERIMENTAL PROCEDURES

Antibodies. Following antibodies were used: monoclonal anti-GBF1 (catalog no. 612116, BD Transduction Laboratories), monoclonal anti-GFP (catalog no. A11120, Invitrogen), monoclonal anti-GFP (catalog no. NBP243575, Novus), polyclonal anti-GFP (catalog no. ab290, Abcam), polyclonal anti-β-COP (catalog no. ab2899, Abcam), monoclonal anti-GM130 (catalog no. 610823, BD Transduction Laboratories). Secondary anti-mouse antibody conjugated to horseradish peroxidase (HRP; catalog no. 1030-05, Southern Biotech). Secondary antibodies conjugated to Alexa 488 and Alexa 594 (catalog nos. A11034, A11029, A11012, A11032; Invitrogen, Madison, WI).

Reagents. Brefeldin A was from Cell Signaling Technology (Beverly, MA). ECL Western blotting reagent was from Thermo Fisher Scientific (Waltham, MA). SuperSignal West Femto Maximum Sensitivity Substrate was from Thermo Scientific (Chicago, IL). Complete protease inhibitor cocktail, EDTA-free, was from Thermo Scientific; 3–12% Blue native (BN)-PAGE gels and molecular weight standards for native gels (catalog no. LC0725) were purchased from Invitrogen.

Plasmids. GBF1/A795E has been described previously (5, 6). All mutations were introduced into GBF1/A795 pcDNA4/To/Myc-His B (Invitrogen) using QuikChange XL Site-Directed Mutagenesis Kit from Agilent Technology. All substitutions were confirmed by sequencing. The sequences of the oligonucleotide primers used for site-directed mutagenesis were: LMK1135AAA/795/GFP (5′-CTGGAGTCACTACAGGAGGCCGCGGCGGCTCTGGTCTCAGTG-3′), RDR1168AAA/795/GFP (5′-GGATTGTGTTGGAGAACGCGGCTGCTGTGGGCTGTGTGTGGC-3′), VLL1-220AAA/795/GFP (5′-GAG ATC AGT GCT CAG GCG GCG GCC TCC CTG CGC ATT TTG C-3′), LF1266AA/795/GFP (5′-AGGTGATGACTGGGCCACAGCCGCCACACTGCTGGAGTGCATCG-3′), L1246R/795/GFP (5′-CAGGTTGCGTATGGGCGCCATGAACTCCTGAAG-3′), L1266E/795/GFP (5′-GTGATGACTGGGCCACAGAGTTCACACTGCTGGAGTG-3′), L1266P/795/GFP (5′-TGACTGGGCCACACCCTTCACACTGCTGG-3′).

Cell culture and transfection. Human HeLa (CCL-2) cells were obtained from ATCC, The Global Bioresource Center. Cells were cultured in vitro in MEM Eagle medium (Cellgro, Manassas, VA) supplemented with L-glutamine, 10% fetal bovine serum, 100 U/ml penicillin, 100 mg/ml streptomycin, and 1 mM sodium pyruvate (Cellgro) at 37°C in a humidified atmosphere. Cells were grown at 37°C in 5% CO_2 in six-well dishes until ~70% confluent and were transfected using Mirus TransIT-LT1 transfection reagent (Mirus Bio, Madison, WI) according to the manufacturer's instructions.

SDS-PAGE and Blue native electrophoresis and Western blotting. For SDS-PAGE, HeLa cells transfected with GFP-tagged GBF1 constructs were lysed in 300 μl of RIPA buffer (150 mM sodium

chloride, 1.0% NP-40, 0.5% sodium deoxycholate, 0.1% SDS, 50 mM Tris, pH 7.4) supplemented with protease inhibitor cocktail by repeated passage through a 26- and 27-gauge needle. The homogenate was centrifuged at 1000 *g* for 15 min at 4°C in a microcentrifuge to remove unbroken cells and nuclei. Proteins were resolved by 8% SDS-PAGE before transfer to NitroPure nitrocellulose membrane (Micron Separations, Westborough, MA) by wet transfer overnight at 30 mV. Membranes were blocked with 5% fat-free milk and probed with antibodies as indicated in each figure. The Western blot band intensity measurements were performed with ImageJ.

For Blue native (BN) electrophoresis, HeLa cells transfected with GFP-tagged GBF1 constructs for ~48 h were lysed using 10% 3-[(3-cholamidopropyl)dimethylammonio]-1-propanesulfonate (CHAPS). Volumes of 15–18 μl of crude protein extract, corresponding to 5 μg of total protein, were loaded on 3–12% BN-PAGE gels and electrophoresis was carried out according to manufacturer's instructions. Following electrophoresis, gels were transferred overnight onto a PVDF membrane at 20 V. Membranes were washed in PBS containing 0.1% Tween 20 (PBS-T) for 8 h, blocked in 5% milk in PBS-T, and then incubated with anti-GFP overnight at 4°C and detected with secondary antibodies conjugated to HRP. The blots were developed using the SuperSignal West Femto Maximum Sensitivity Substrate, according to the manufacturer's directions.

Imaging. HeLa cells were seeded overnight on glass coverslips, transfected and ~18 h later processed for immunofluorescence. In some experiments, transfected cells were washed in phosphate-buffered saline (PBS) and incubated with 0.5 μg/ml brefeldin A (BFA) for 30 min at 37°C before processing. Cells were washed in PBS, fixed in 3% paraformaldehyde for 10 min, and quenched with 10 mm ammonium chloride. Cells were permeabilized with 0.1% Triton X-100 in PBS. The coverslips were then washed with PBS and blocked in PBS containing 2.5% goat serum, 0.2% Tween 20 for 5 min followed by blocking in PBS containing 0.4% fish skin gelatin, and 0.2% Tween 20. Cells were incubated with primary antibodies for 1 h at room temperature. Coverslips were washed with PBS containing 0.2% Tween 20 and incubated with secondary antibodies for 45 min. Nuclei were stained with Hoechst dye. Coverslips were washed as described above and mounted on slides in ProLong Gold antifade reagent (Invitrogen). Fluorescence patterns were visualized using a Leitz Wetlzar microscope with epifluorescence and Hoffman Modulation Contrast optics by Chroma Technology (Bellows Falls, VT). Images were captured with a 12-bit CCD camera from QImaging (Surrey, BC, Canada) and processed with iVision-Mac software.

Confocal imaging was on a PerkinElmer Ultraview ERS 6FE spinning disk attached to a Nikon TE 2000-U microscope. The system was equipped with laser and filter sets to visualize and image FITC, TRITC, and DAPI fluorescence. Images were captured using a Hamamatsu C9100-50 EMCCD camera (Hamamatsu Photonics, Hamamatsu city, Japan) and ×60 or ×100 Plan APO oil-immersion objectives. The imaging system was operated by Volocity 6.2 software (PerkinElmer, Shelton, CT).

Colocalization quotients. At least 20 transfected cells perimeters were selected for each condition, and the Pearson coefficient between GBF1 (green) and GM130 (red) localization was calculated by ImageJ. The dispersion graph data was represented as absolute values, where each dot corresponds to one transfected cell.

Quantification of Golgi intactness. At least 50 transfected cells were quantified for each condition, where their Golgi architecture status was checked by labeling with anti-GM130 and classified as undisrupted (intact) or disrupted (diffuse). The data are represented as percentage of the total transfected cells showing undisrupted Golgi.

Secretion assay. HeLa cells were cotransfected in 96-well plates with plasmids encoding *Gaussia* luciferase (GLUC) and a GBF1 construct (1:9 mass ratio). An empty vector was used instead of a GBF1-coding plasmid as a negative control, while GBF1/795 construct was used as a positive control. The next day, the medium was removed, and the cells were washed to remove secreted luciferase and incubated in 25 μl of fresh medium supplemented with the indicated amount of BFA. After 4 h of incubation, the medium was transferred into another 96-well plate, and the amount of secreted luciferase was measured with BioLux *Gaussia* luciferase assay kit (New England BioLabs) according to the manufacturer's recommendations.

Viability assay. HeLa cells were transfected with GFP-tagged GBF1 constructs for ~18 h. The next day, the medium was replaced with fresh medium containing 0.5 μg/ml BFA and the cells were lysed with RIPA and processed by SDS-PAGE and Western blotting immediately ($t = 0$), after 8 h ($t = 8$), or after 24 h.

Bioinformatics. Multiple sequence alignment was performed using ClustalW (24, 29). α-Helices were predicted using JPred3 (19).

RESULTS

Targeting conserved amino acids in the HDS2 domain of GBF1. In addition to the highly conserved Sec7d present in all ARF GEFs, GBF1 contains five additional domains (DCB, HUS, HDS1–3) that show significant sequence conservation in GBF1 orthologs from various phyla (Fig. 1*A*) (12). Herein, we focus on the HDS2 domain located within the COOH-terminal two-thirds of GBF1 and composed of amino acids 1098 to 1277. The ~280-amino acid HDS2 domain is predicted (the structure of HDS2 is currently unknown) to contains six α-helices, each with regions of significant sequence homology across the phylogenetic tree (Fig. 1*B* shows amino acid conservation between human, zebrafish, and fruit fly GBF1 orthologs) (12, 68). High level of sequence conservation during evolution is often indicative of catalytic motifs or other key protein-protein interfaces. However, the role of the conserved residues within the HDS2 domain in the functionality of GBF1 has not been characterized. Thus, we created alanine substitutions in HDS2 residues that were highly conserved in terms of identity and location within the predicted secondary structure, as determined by multiple sequence alignments and secondary structure predictions (Fig. 1, *C–F*) (12). The residues selected for alanine substitution were LMK1135–1137 in α-helix 1 (to generate the LMK variant), RDR1168-1170 in α-helix 2 (to generate the RDR variant), VLL1220-1222 in α-helix 4 (to generate the VLL variant), and LF1266-1267 in α-helix 6 (to generate the LF variant) (Fig. 1*B*; boxed in red). In addition, single amino acid substitutions were used to generate L1268E (called E) and L1266P (called P) variants. All these mutations are distinct from the L1246R mutation (called LR) in α-helix 5 studied before (Fig. 1*B*; residue boxed and indicated in red) (13).

Mutations in the HDS2 domain impair GBF1 ability to maintain Golgi architecture. It is currently unknown whether an intact HDS2 domain is required for cellular functions of GBF1. Assessing the functionality of mutant proteins in cells containing the endogenous protein is difficult, and unless the mutant protein acts as a dominant negative, the loss of function is not observable. To overcome this, we utilized a functional "replacement" assay. We first introduced the A795E mutation within the catalytic Sec7d of wild-type GBF1 and each of our GBF1 mutants (Fig. 1*A*). The alanine at position 795 is immediately adjacent to the catalytic "glutamic finger" at position 794 and contributes to the binding site for the inhibitor BFA, which binds to an interface of a GEF complexed to its substrate ARF (40, 54). Mutating the alanine 795 to a glutamic acid (A795E) sterically hinders BFA binding and, hence, renders all constructs containing the A795E substitution resistant to BFA

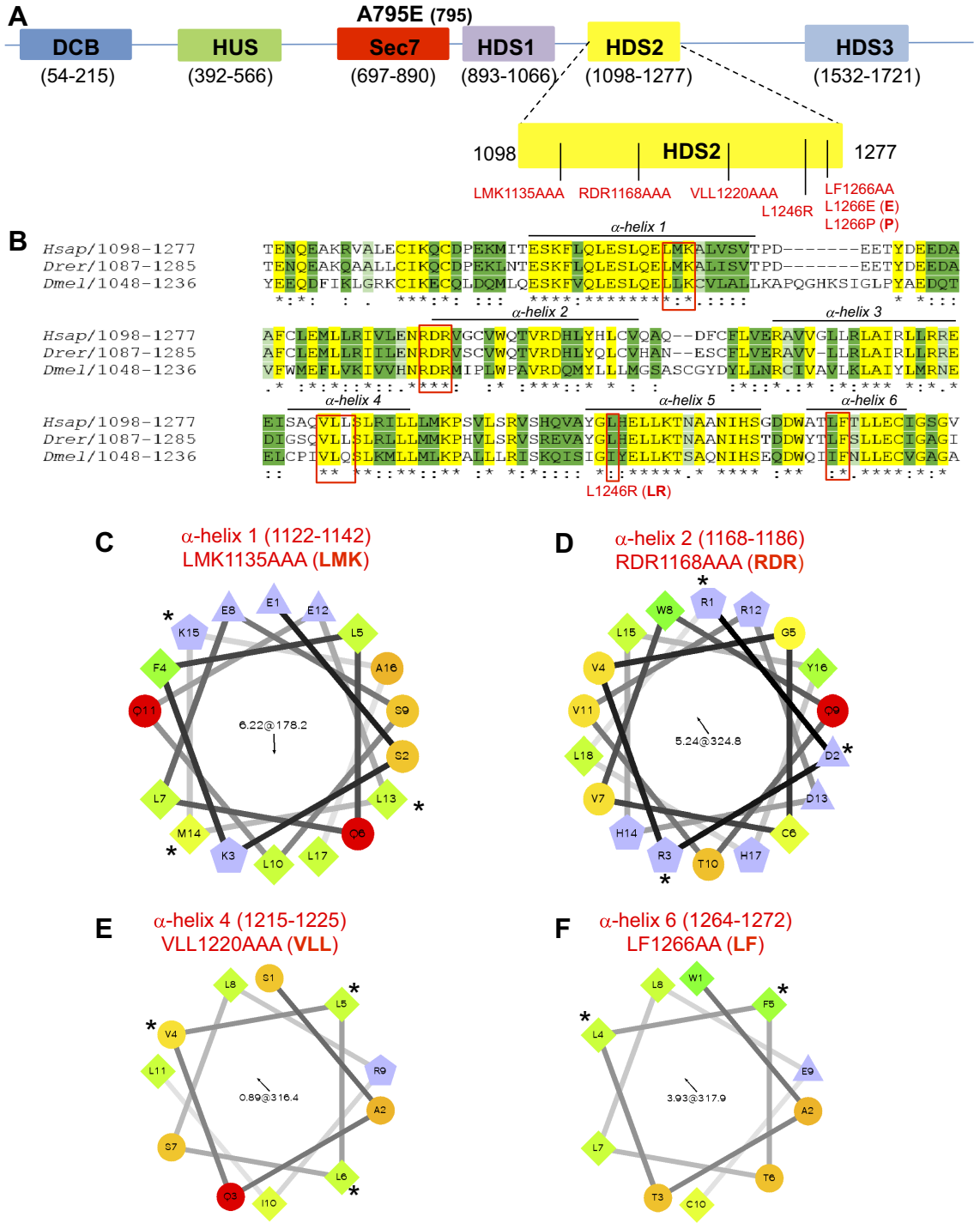

Fig. 1. Mutations in HDS2 (homology downstream of Sec7 domain 2) of Golgi brefeldin A-resistant factor 1 (GBF1) analyzed in this study. *A*: schematic representation of full-length GBF1 showing overall domain organization and location of mutations within the HDS2 domain analyzed in this study. The A795E mutation within the Sec7d that confers brefeldin A (BFA) resistance is indicated. *B*: HDS2 sequences for *Homo sapiens* GBF1 (*Hsap*; AAI17683.1) and GBF1 orthologs from *Danio rerio* (*Drer*; XP_009305378.1) and *Drosophila melanogaster* (*Dmel*; NP_725133.1) retrieved from GenBank were aligned using Clustal Omega. Identical amino acids are shaded in yellow and indicated by asterisks below the sequences. Strongly similar amino acids are indicated by dark green shading and a colon below the sequences. Weakly similar amino acids are indicated by light green shading and a period below the sequences. Predicted α-helical regions are indicated by black lines above the sequences. *C–F*: helical wheel projections of the 4 α-helices analyzed in this study with the mutated residues indicated with asterisks. Hydrophilic residues are circles, hydrophobic residues are squares, potentially negatively charged residues are triangles, and potentially positively charged residues are pentagons. The most hydrophobic residues are green, the amount of green decreasing proportionally to the hydrophobicity, with zero hydrophobicity coded as yellow. Hydrophilic residues are red, with pure red being the most hydrophilic (uncharged) residue and the amount of red decreasing proportionally to the hydrophilicity.

(5, 6, 15, 40, 54). Thus, the A795E-containing wild-type GBF1 can rescue cells from BFA sensitivity when expressed in cells in which the endogenous GBF1 is inhibited by BFA (6, 9). Such functional rescue forms the basis of a cellular replacement assay in which the GBF1/A795E constructs containing mutations within the HDS2 domain can be expressed in cells in which the endogenous GBF1 is acutely inactivated with BFA, and their ability to support functions normally performed by GBF1 can be assessed by biochemical and imaging approaches. All GBF1 constructs used in the functional assays in this study contain the A795E substitution and are BFA resistant (all are designated 795). In addition, all constructs are tagged at the NH_2 terminus with GFP. We have shown previously that such tagging doesn't influence GBF1 functionality (1, 23, 64).

Because we planned to compare the behavior of different GBF1 mutants, we first ensured that expression levels and transfection efficiency of the constructs were analogous and that any observed phenotypes were not due to differential expression of the constructs. HeLa cells were mock-transfected or transfected with GFP-tagged GBF1/795 (795), LR, LMK, RDR, VLL, LF, E, and P for ~18 h and then either lysed, and the lysates processed for SDS-PAGE and Western blotting to quantitate expression levels, or processed for immunofluorescence with anti-GFP to quantitate the transfection efficiency.

Analogous levels of expression were seen for all tested constructs (Fig. 2, *A–C*). As shown in Fig. 2*A*, only the endogenous GBF1 (band at ~200 kDa) was visible in the mock-transfected cells, while an additional band at ~230 kDa was visible in lysates from transfected cells. The identity and quantity of each construct were confirmed by probing with anti-GFP (Fig. 2*B*). Similar levels of each construct were detected relative to the GM130 loading control (Fig. 2*C*), indicating that any observed functional differences between the constructs were not due to lack of expression. This analysis also suggests that the mutant GBF1 species were not significantly different in terms of their stability, implying that all might be correctly folded. To assess the overall folding of HDS2 constructs, we compared the mutants to the 795 construct by Blue native (BN) gel electrophoresis. We (9) had shown previously that endogenous GBF1 and 795 migrate as an ~880-kDa species on BN gels. In agreement, 795 was detected at ~880-kDa (Fig. 2*D*). Importantly, all tested GBF1 variants with mutations in the HDS2 domain also migrated at ~880 kDa, suggesting overall folding and oligomerization analogous to that of wild-type GBF1.

Similarly, the transfection efficiency was similar for all the constructs with means ± SE of 51.3% ± 0.94 for 795, 48.02% ± 0.73 for LR, 50.78% ± 1.08 for LMK, 45.75% ± 0.47 for RDR, 42.78 ± 1.65 for VLL, 48.12% ± 6.87 for LF, 52.12% ± 0.57 for E, and 43% ± 0.61 for P (Fig. 2, *E–L*, and images not shown).

In the vast majority of mammalian cells (including HeLa), the Golgi complex has a characteristic crescent shape that reflects the stacked arrangement of cisternae within the perinuclear region surrounding the microtubule-organizing center (30, 36, 44, 47, 48, 55, 57, 69). A key cellular function of GBF1 is the maintenance of this typical Golgi architecture. Molecular or genetic depletion of GBF1, or inhibition of GBF1 catalytic activity with pharmacological drugs (BFA, Golgicide or LG186), results in extensive tubulation and the ultimate collapse of the Golgi into the ER (2, 10, 23, 32, 56, 62, 64, 67, 72, 73). To assess the ability of our HDS2 mutants to maintain Golgi architecture, we used the functional replacement assay. HeLa cells were transfected with 795, LR, LMK, RDR, VLL, LF, E, or P for ~18 h, treated with BFA (0.5 μg/ml for 30 min) to inactivate the endogenous GBF1, and then proceed by immunofluorescence with anti-GFP to detect transfected cells, and anti-GM130 (42) to assess Golgi integrity.

As expected, cells expressing the 795 construct had GM130 in the characteristic Golgi structure in the perinuclear region, whereas untransfected cells had GM130 in disrupted Golgi elements scattered throughout the cells (Fig. 2*E*). Similarly, cells expressing the LMK (Fig. 2*G*) or the VLL (Fig. 2*I*) construct showed characteristic Golgi structure in the perinuclear region. In contrast, the Golgi elements in cells expressing the LR (Fig. 2*F*), RDR (Fig. 2*H*), or the LF (Fig. 2*J*) constructs were more fragmented and not as concentrated in the perinuclear region. An intermediate Golgi phenotype is seen in cells expressing the E (Fig. 2*K*) or the P (Fig. 2*L*) constructs.

The ability of each construct to sustain compact Golgi architecture was quantitated based on their fragmentation pattern. We show representative images of our scoring parameters, with undisrupted Golgi considered as a largely cohesive single structure (Fig. 2*M*) and disrupted Golgi considered as an assembly of scattered separate elements dispersed away from each other (Fig. 2*N*). Blinded quantification (the scorers were unaware of the construct they were scoring) indicated that the 795 and the LMK constructs supported compact perinuclear Golgi in ~85% of transfected cells, whereas the VLL supported Golgi architecture in ~80% of the transfected cells (Fig. 2*O*). The singly substituted E and P mutants showed lower ability to support Golgi homeostasis but still maintained intact Golgi in ~60% of transfected cells. In contrast, the previously described inactive LR mutant supported Golgi homeostasis in only ~5% of the transfected cells. The RDR construct supported Golgi architecture in ~40% of transfected cells, whereas the LF construct was the least functional of the new HDS2 mutants, and supported Golgi homeostasis in only ~35% cells. Intact Golgi were observed in only ~5% of untransfected cells, indicating that even the most compromised of our new GBF1 mutants remained at least partially functional in this assay. However, our results indicate that an intact RDR1168 in α-helix 2 and an intact LF1266 in α-helix 6 are required for GBF1 to be fully functional.

Effect of HDS2 mutations on GBF1-mediated COPI recruitment. Golgi homeostasis requires the formation of COPI vesicles and COPI-mediated traffic, and treatments that deplete COPI components or prevent membrane association of the COPI coatomer cause Golgi disruption (1, 20, 31, 58, 60). COPI recruitment requires GBF1-mediated ARF activation, and we assessed the ability of the different HDS2 mutants to recruit COPI to Golgi membranes as a read-out of their ability to activate ARF.

HeLa cells were transfected with 795, LMK, RDR, VLL, or LF for ~18 h, treated with BFA (0.5 μg/ml, 30 min) to inactivate endogenous GBF1 and then processed to detect transfected cells (with anti-GFP) and COPI recruitment (with anti-β-COP). As expected, cells expressing the 795 construct recruit COPI to the characteristic Golgi structures in the perinuclear region (Fig. 3*A*). Similarly, Golgi-associated COPI is detected in cells expressing the LMK (Fig. 3*B*) or the VLL (Fig. 3*D*) constructs. A much more diffuse localization of

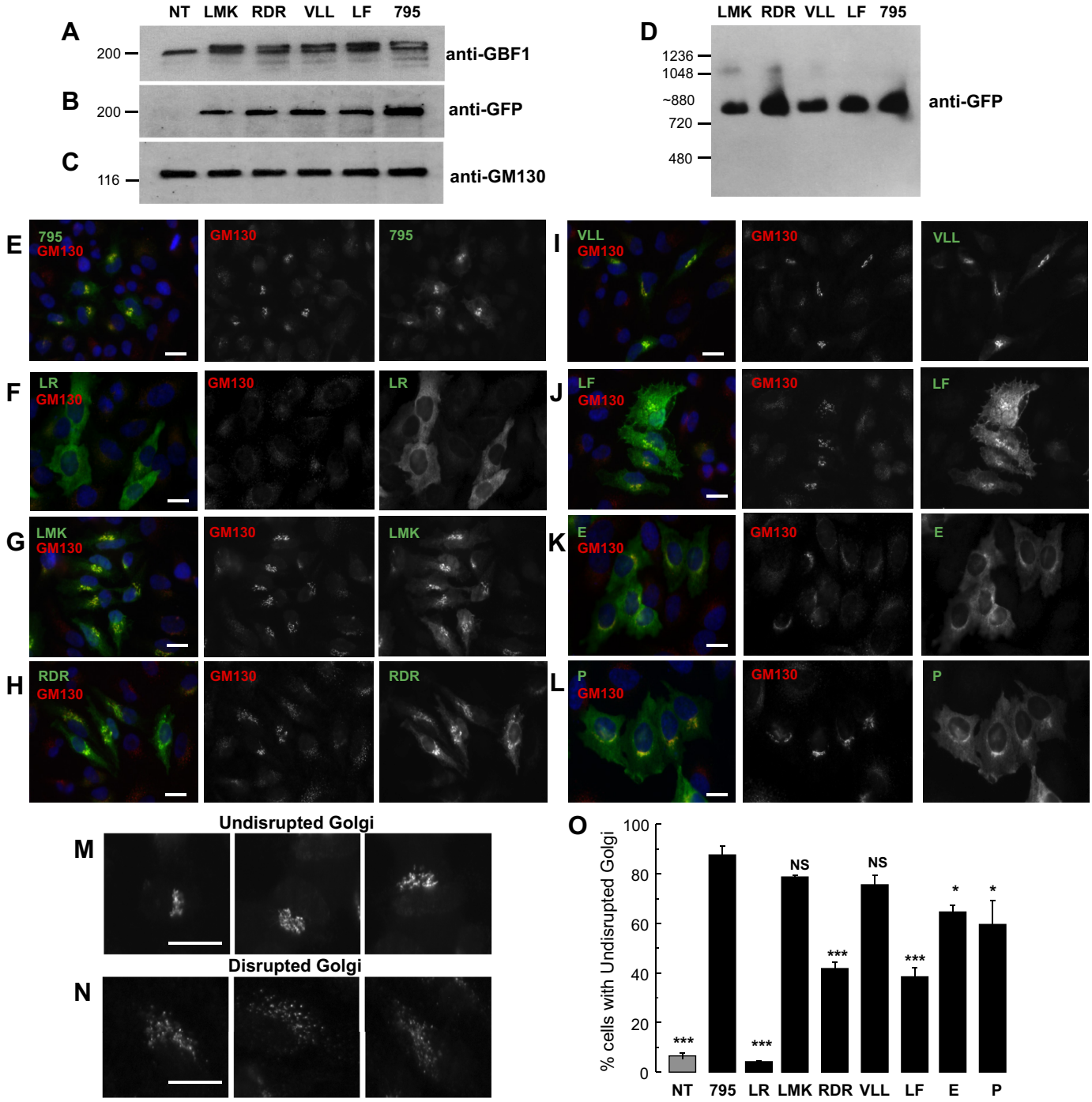

Fig. 2. Intact HDS2 is required for GBF1 function in Golgi homeostasis. *A–C*: lysates from HeLa cells transfected with the indicated constructs (all tagged at the NH_2 terminus with GFP) were analyzed by SDS-PAGE and Western blotting with indicated antibodies. Similar levels of each construct are detected. *D*: cells transfected with the indicated constructs (all tagged at the NH_2 terminus with GFP) were lysed without detergent and the lysates analyzed on Blue native (BN) gels, followed by Western blotting with anti-GFP. HDS2 mutants migrate in a manner analogous to that of GBF1/795. *E–L*: HeLa cells were transfected with the indicated GFP-tagged GBF1 construct and grown overnight. Cells were then treated with 5 μg/ml BFA for 30 min and processed by immunofluorescence with anti-GFP (to detect transfected cells) and anti-GM130 (to assess Golgi architecture). A merged image is shown at *left*; GM130 alone is shown at *right*. Bars, 10 μm. *M* and *N*: representative images of cells containing compact perinuclear Golgi structures and classified as undisrupted Golgi (*M*) and cells containing multiple dispersed fragments and classified as disrupted Golgi (*N*). Bars, 10 μm. *O*: images analogous to those in *E–L* were analyzed, and %transfected cells containing intact Golgi were quantitated. Data represent means ± SE of 3 independent experiments (>50 cells counted per experiment). The means were compared with the control condition (cells expressing GBF1/795) by Dunnett test (*$P < 0.05$, ***$P < 0.001$; NS, not significantly different). Constructs containing substitution at the L1246, RDR1168 or the LF1266 position in HDS2 are compromised in maintaining Golgi homeostasis.

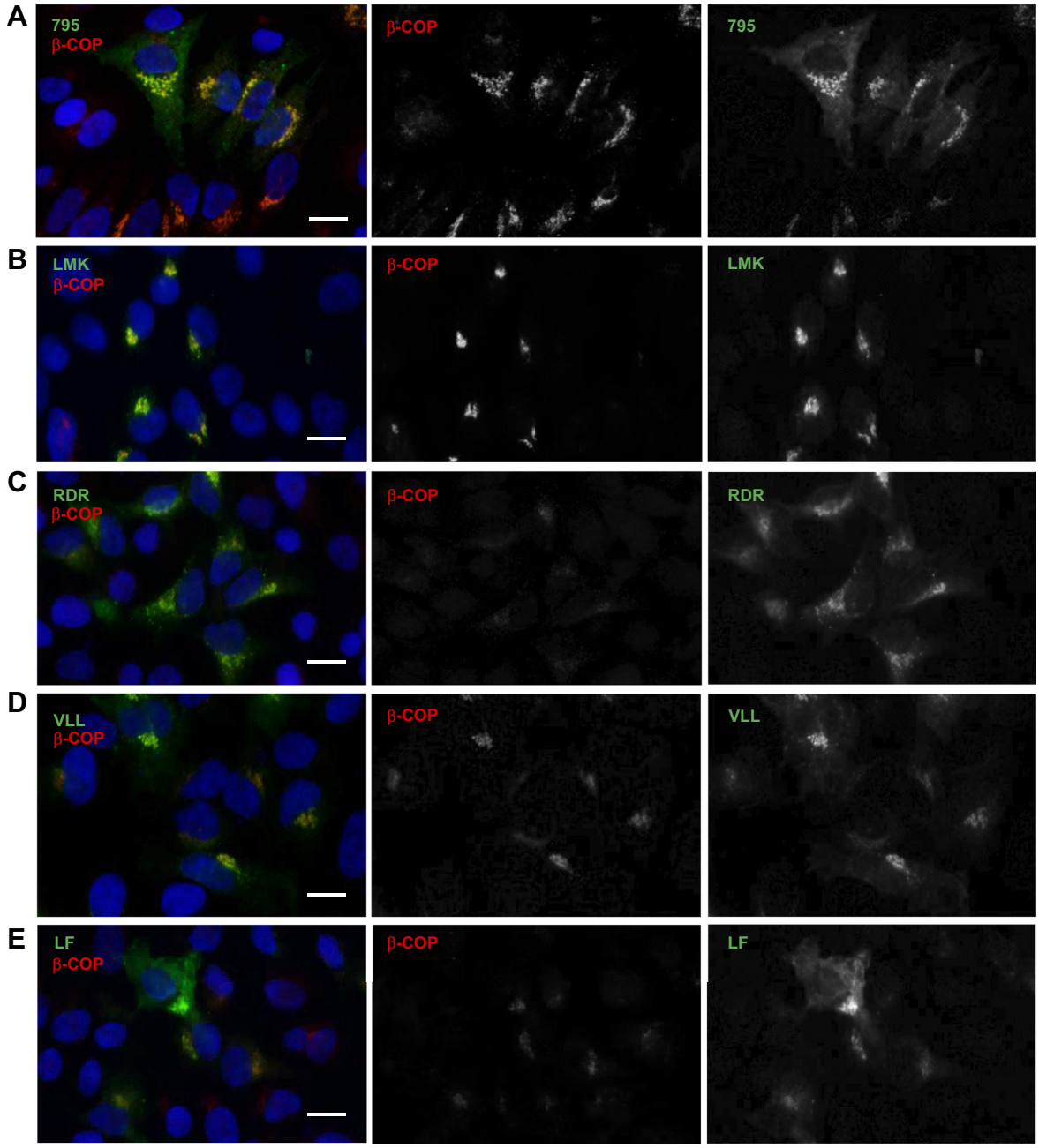

Fig. 3. Mutations within HDS2 of GBF1 affect COPI recruitment. *A–E*: HeLa cells were transfected with the indicated GFP-tagged GBF1 constructs and grown overnight. Cells were then treated with 5 μg/ml BFA for 30 min and processed by immunofluorescence with anti-GFP (to detect transfected cells) and anti-β-COP (to assess COPI recruitment as a readout for ADP-ribosylation factor (ARF) activation). A merged image is shown at *left*; the β-COP alone image is shown at *right*. Constructs containing substitution at the RDR1168 or the LF1266 position in HDS2 are impaired in ARF activation required for COPI recruitment to the Golgi. Bars, 10 μm.

COPI is detected in cells expressing the RDR (Fig. 3*C*), and even more diffuse recruitment is observed in cells expressing the LF (Fig. 3*E*) mutant. However, even in cells with the most dispersed Golgi, we still detected some COPI recruitment, suggesting that even the most compromised HDS2 mutants are at least partially functional in ARF activation.

Mutations in the HDS2 domain impair GBF1 ability to sustain secretion. The data above suggest that our RDR and the LF mutants are compromised in their ability to maintain compact Golgi architecture but do not address whether such disrupted Golgi may retain secretory capacity. A perinuclear ribbon-like structure of the mammalian Golgi is not required to sustain secretion and cell life, since cells treated with nocodazole to depolymerize microtubules and fragment the Golgi are still capable of secretion (53, 66). Similarly, cells of non-mammalian species, such as *Drosophila melanogaster, Caenorhabditis elegans*, and all plant species have dispersed Golgi yet are efficient in secretion (4, 22, 62). Thus, we assessed the ability of the HDS2 mutants to support the secretion of the Gaussia luciferase containing a natural signal sequence that

targets it to the ER and allows its passage through the secretory pathway and release from cells (65).

HeLa cells were cotransfected with a plasmid encoding Gaussia luciferase and LR, LMK, RDR, VLL, LF, E, or P. The 795 construct and an empty vector were used as a positive and a negative control, respectively, within each experimental set to control for any possible variability between data sets. The next day the medium was removed, and the cells were washed to remove secreted luciferase and then incubated in fresh medium containing 0.5 μg/ml BFA. The BFA inhibits the endogenous GBF1, leaving the exogenously expressed GBF1 constructs as the sole BFA-resistant GBF1 species in the cell. After 4 h of incubation, the medium was collected and the level of secreted luciferase assayed.

As shown in Fig. 4, empty vector bars, cells transfected with the luciferase-expressing plasmid, and an empty vector are almost completely inhibited in secretion at the BFA concentration tested. In contrast, cells expressing the luciferase and the 795 construct (Fig. 4, *A–G*; 795 bars) remain capable of ~70% secretion when treated with BFA. Cells expressing the LMK construct are also capable of secretion, with ~70% secretion still supported after BFA treatment (Fig. 4*B*). Similarly, cells expressing the VLL construct secrete well, with ~75% secretion after BFA (Fig. 4*D*). Cells transfected with E and P mutants secrete similarity well, with ~60% secretion after BFA (Fig. 4, *F* and *G*). In contrast, cells expressing the LR mutant were impaired in secretion, with ~10% secretion observed after BFA addition (Fig. 4*A*). The RDR construct also is impaired in secretion, with only ~40% secretion maintained (Fig. 4*C*). This indicates that the RDR1168 motif is important for GBF1 function in secretion. However, this level of secretion is still higher than the ~5% secretion observed in cells expressing the empty vector in this data set. Cells expressing the LF mutant show the most severe defect in secretion among the new HDS2 mutants, maintaining only ~25% of secretion after BFA addition (Fig. 4*E*). This value is not much different from the ~20% secretion efficiency seen in this data set for cells expressing luciferase and an empty vector. These results suggest that an intact LF1266 motif in α-helix 6 is absolutely essential for the secretory function of GBF1.

HDS2 domain regulates GBF1 targeting to the Golgi. GBF1 is a cytosolic protein that rapidly cycles on and off Golgi membranes (46, 63). GBF1 facilitates ARF activation only while membrane associated, implying that membrane recruitment of GBF1 provides a regulatory hotspot for modulating the cellular activity of GBF1. Deletion of the entire HDS2 from GBF1 has been shown to prevent Golgi localization, but whether the lack of association was due to the possible misfolding of the deleted construct was not determined (11). Furthermore, the identity of the structural elements within HDS2 required for Golgi targeting were not examined. Thus, to define the motifs within the HDS2 domain required for Golgi association, we compared the efficiency of Golgi targeting of our constructs. HeLa cells were transfected with 795, LR, LMK, RDR, VLL, or LF for ~18 h and then processed by immunofluorescence with anti-GFP (to detect the construct) and anti-GM130 (to identify the Golgi). As shown in Fig. 5, *A–F*, all constructs show partial colocalization with the GM130 Golgi marker, indicating that all are capable of at least partial Golgi targeting. Quantification of the targeting efficiency (Fig. 5*G*) shows that 795, LMK, and VLL target efficiently to the Golgi (shown by the high Pearson coefficient with GM130). In contrast, LR shows extremely poor targeting, while RDR and LF are also compromised, although to a lesser extent. These data indicate that mutations within the α-helix 2 and the α-helix 6 of HDS2 decrease the ability of GBF1 to target to the Golgi membrane.

Mutations in HDS2 impair GBF1 ability to sustain cell viability. Secretion is an essential cellular function, and inhibiting secretion through pharmacological treatments or molecular and genetic means causes cell death. Specifically, inhibiting secretion with BFA induces ER stress and the unfolded protein response (UPR) and ultimately leads to cell death through apoptosis (17). Such BFA-induced cytotoxicity can be used as a means to assess the functionality of our BFA-resistant constructs. We selectively focused on the previously shown to be inactive LR mutant, and our new mutants containing alanines in place of RDR1168 or LF1266, since substituting those residues with alanines appears to most dramatically reduce GBF1 function. To provide a goalpost for the amount of cell killing in the absence of functional GBF1, we also assessed the viability of cells expressing the wild-type GBF1 (wild-type GBF1 is BFA sensitive). To provide a goalpost for the level of cell death in the presence of functional GBF1, we measured the viability of cells expressing the BFA-resistant 795.

HeLa cells were transfected with GFP-tagged wild-type GBF1 (BFA sensitive), 795, LR, RDR, or LF for ~18 h and then treated with BFA (0.5 μg/ml) for 0, 8, or 24 h to inactivate endogenous GBF1. At each time point, the cells were washed to remove dead cells, and the remaining cells were lysed. The lysates were then processed by SDS-PAGE and Western blotting with anti-GM130 to determine the level of general cell loss, and with anti-GFP to determine the loss of cells expressing a particular GBF1 construct. We expected that cells expressing functional GBF1 survive the BFA treatment and that the lysate from such cells will have a higher GFP signal to the GM130 signal after 24 h than at 0 h, whereas cells expressing non-functional GBF1 die at the same rate as untransfected cells, leading to a parallel loss of the GFP and the GM130 signal.

Wild-type GFP-GBF1 was detected at 0 and 8 h of BFA treatment, but we did not detect a signal after 24-h BFA treatment, indicating the almost complete loss of the cells expressing this construct (Fig. 6*A*, WT panel). In contrast, the levels of the 795 construct remained almost unchanged at 0, 8, and 24 h of BFA treatment, indicating that cells expressing this construct remained viable due to the functional GBF1 (Fig. 6*A*, 795 panel). The RDR construct was also detected at 0, 8, and 24 h (although decreased at 24 h), suggesting that the cells expressing this construct survived the BFA treatment (Fig. 6*A*, RDR panel). In contrast, the LR construct was detected at 0 and 8 h but was significantly decreased after 24 h (Fig. 6*A*, LR panel). Similarly, the LF construct was detected at 0 and 8 h but was lost at 24 h, indicating the loss of cells expressing this construct (Fig. 6*A*, LF panel).

Densitometric analyses of gels analogous to those in Fig. 6*A* indicate that only ~35% of cells expressing the wild-type BFA-sensitive GFP-GBF1 persisted after 24 h of BFA treatment, whereas ~80% of cells expressing 795 were still present after the 24-h BFA treatment (Fig. 6*B*). Cells expressing the LR construct died almost as readily as those not having a functional GBF1, with only ~40% remaining after 24 h. Cells

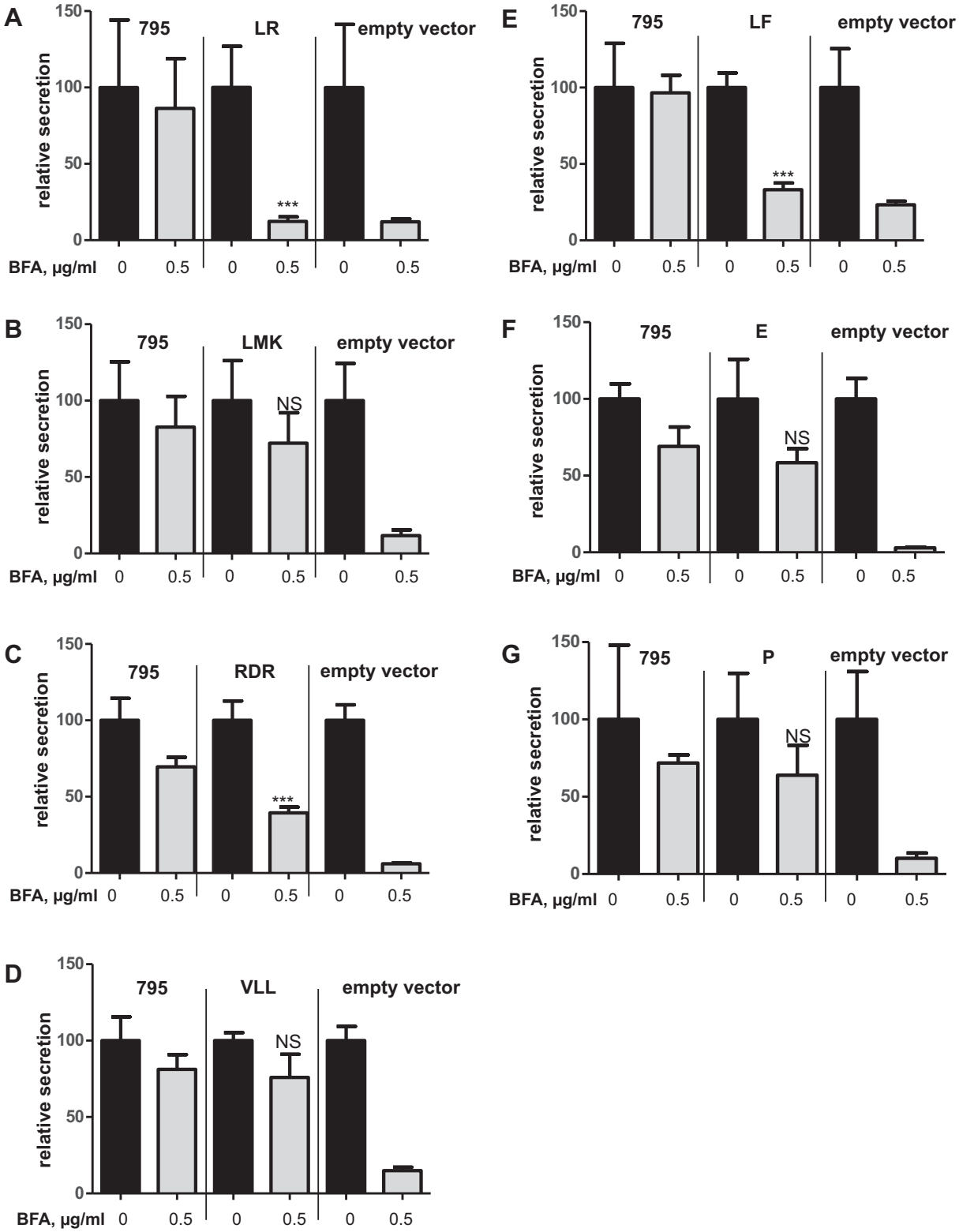

Fig. 4. Mutations within HDS2 affect GBF1 function in secretion. *A–G*: HeLa cells were cotransfected with pCMV-GLUC encoding *Gaussia princeps* luciferase and either an empty vector or the indicated plasmid and grown overnight. The next day, cells were washed with serum-free medium to get rid of the already secreted luciferase and placed in fresh growth medium containing 0.5 μg/ml BFA for 4 h. Amount of luciferase secreted into medium was then measured. Signal from at least 8 wells was averaged for each sample. Data represent means ± SE of 8 independent secretion assays. Means were compared with cells expressing GBF1/795 by unpaired two-tailed *t*-test (***$P < 0.001$). Constructs containing substitution at the L1246, RDR1168 or the LF1266 position in HDS2 are impaired in secretion.

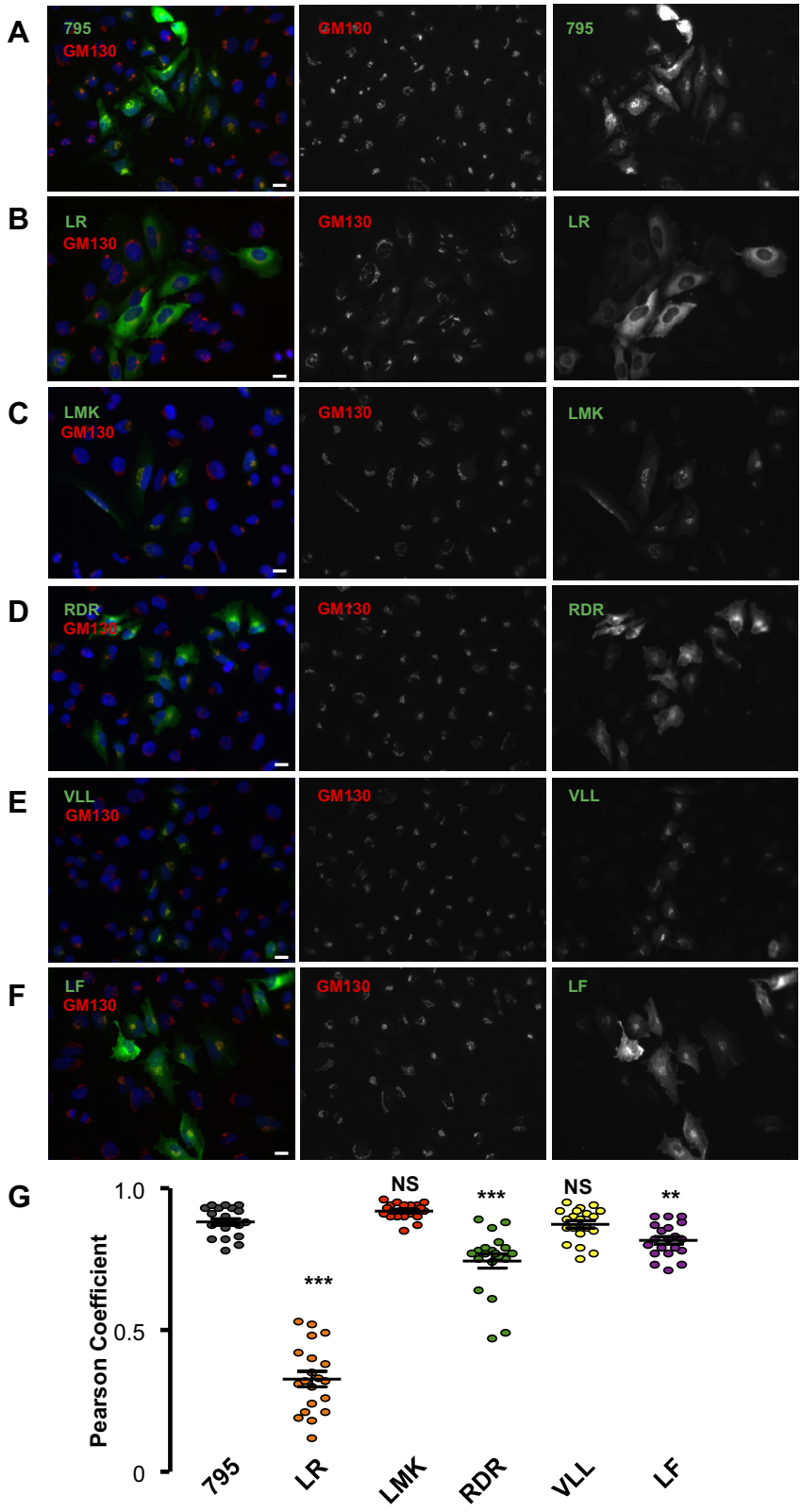

Fig. 5. Mutations within HDS2 decrease GBF1 targeting to the Golgi. *A–F*: HeLa cells were transfected with the indicated GFP-tagged GBF1 constructs and grown overnight. Cells were then processed by immunofluorescence with anti-GFP (to detect GBF1 constructs) and anti-GM130 (to assess Golgi targeting). Merged images are shown. Bars, 10 μm. *G*: amount of each GBF1 construct in >20 transfected cells that colocalized with GM130 (Golgi) was assessed and is represented as an individual Pearson coefficient. Means were compared with the control condition (cells expressing GBF1/795) by nonparametric multiple comparison (Dunnett test equivalent; $^{**}P < 0.01$, $^{***}P < 0.001$). GBF1 variants containing substitution at the LR1246, RDR1168 or LF1266 positions in HDS2 appear impaired in associating with Golgi membranes.

expressing the RDR mutant were partially protected, and ~55% of cells expressing this mutant were still present after the 24-h BFA treatment. In contrast, only ~10% of cells expressing the LF mutant persisted after the BFA treatment. These results suggest that the RDR mutant is partially functional, in agreement with its ability to partially support Golgi homeostasis and secretion, whereas the LF mutant lacks the ability to support the essential functions required for cellular life that are normally fulfilled by GBF1. These data indicate that mutations within the α-helix 2 and the

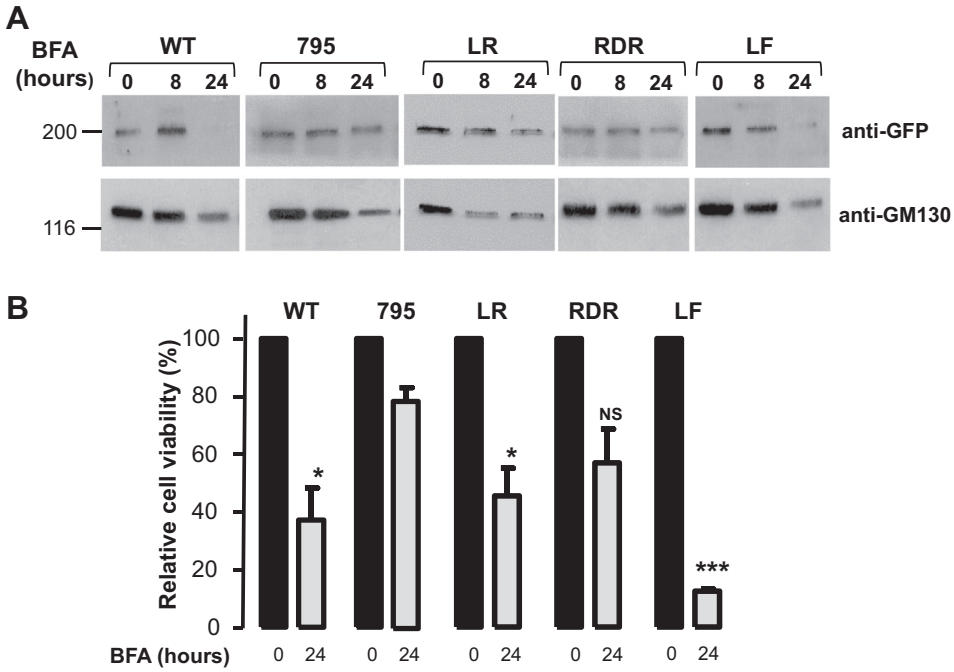

Fig. 6. Mutations within HDS2 inhibit GBF1 function essential for cell viability. *A*: HeLa cells expressing the indicated GFP-tagged constructs for ~18 h were incubated with 0.5 μg/ml BFA for 0, 8, or 24 h, washed to remove dead cells, and then lysed. Lysates were analyzed by Western blotting with anti-GM130 to estimate the proportion of total cells remaining, and with anti-GFP to estimate the proportion of cells expressing each construct remaining after BFA treatment. *B*: gels analogous to that in *A* were quantitated by densitometry, and data are presented as % of each construct remaining after 24-h BFA treatment relative to *time 0*. Data represent means ± SE of 2 independent experiments. Means were compared with cells expressing GBF1/795 by unpaired two-tailed *t*-test (*$P < 0.05$, ***$P < 0.001$). Cells expressing GBF1 variants containing substitution at the L1246 or the LF1266 positions in HDS2 are compromised in supporting cell viability.

α-helix 6 of HDS2 strongly affect the ability of GBF1 to support cellular viability.

DISCUSSION

The ARF family of small Ras-related GTPases contains key regulators of essential cellular processes, including ARFs that control membrane traffic within the secretory and endosomal pathways. Like all GTPases, ARFs cycle between an inactive GDP-bound state found within the cytosol and a GTP-bound active state bound to membrane bilayers. The activation occurs through GDP/GTP exchange, and in cells is catalyzed by a subfamily of Sec7d-containing GEFs that include GBF1 and the closely related BIG1 and BIG2. ARF activation requires structural rearrangements within the ARF that can occur in cells only within the framework of the cytosolic leaflets of membrane bilayers (7, 52). Thus, to activate ARFs, the GEFs must be positioned on membranes. All GEFs are soluble cytosolic proteins that are recruited to membranes in repeated cycles of binding and dissociation to initiate ARF activation in a spatio-temporally restricted manner. Membrane binding of GEFs is required for ARF activation, implying that mechanisms that regulate GEF recruitment to compartments also regulate ARF–mediated downstream events. Thus, membrane binding of GEFs must be tightly regulated to restrict ARF activation to specific sites and times. In addition, GEF's interactions with membranes are often coupled to the activation of the catalytic activity of the GEF through distinct allosteric mechanisms (reviewed in Ref. 43).

Our understanding of mechanisms that target and activate the Sec7d-containing GEFs to membranes is uneven. We have a considerable body of knowledge on the mechanisms that facilitate the recruitment and the activation of the small GEFs belonging to the cytohesin, BRAG and F-box families at the plasma membrane and endocytic compartments, and on the involvement of the pleckstrin homology (PH) domains found in this class of GEFs in the recruitment and activation. In contrast, our insight into how the GBF1/BIG1/2 subfamily is recruited to the ERGIC, the Golgi and the TGN/endosomal membranes is limited. Importantly, GBF1/BIG1/2 do not contain PH domains; thus, their membrane recruitment and activation must occur through different mechanism(s).

The NH_2-terminal region of GBF1 (20, 34) appears required for Golgi targeting, as the deletion of the NH_2-terminal 37 amino acids of GBF1 prevents membrane association (38). The NH_2-terminal 384 residues of GBF1 have been shown to bind Rab1b, and this interaction promotes GBF1 membrane association, since overexpression of the active form of Rab1b promotes GBF1 recruitment, whereas depletion of Rab1b leads to decreased GBF1 association (39). However, additional interactions of GBF1 participate in Golgi recruitment, since even almost complete depletion of Rab1b does not prevent GBF1 from targeting to the Golgi. Thus, GBF1 targeting appears to be multifaceted, and previous studies have shown that deletion of the HDS1 or the HDS2 domains (individually or in tandem) also inhibits GBF1 targeting to Golgi membranes (11). The importance of the HDS2 domain was confirmed by studies showing that the L1246R missense mutation within the HDS2 α-helix 5 of the zebrafish GBF1 ortholog prevents its membrane association (13). However, which structural motifs within the HDS2 domain participate in GBF1 membrane association and whether they might control distinct aspects of GBF1 cellular function have not been examined. Thus, we undertook a rational and comprehensive analysis of HDS2 structure-function relationships to identify the parameters regulating GBF1 targeting to Golgi membranes and controlling its cellular function.

We generated a number of GBF1 variants in which select, highly conserved residues within the distinct α-helices of HDS2 were substituted with alanines, prolines, or glutamic acid. The HDS2 domain contains six α-helices and we targeted α-helices 1, 2, 4, and 6 [the effect of a mutation within α-helix 5 has been reported previously (13)]. We preferentially chose

charged and/or hydrophobic residues within each α-helix for alanine substitutions (Fig. 1). The substitutions did not appear to disrupt the overall folding of the GBF1 variants, since all were expressed efficiently in cells, were stable, and exhibited correct oligomeric state (Fig. 2) (aberrantly folded proteins tend to be degraded in cells and often are incapable of correct oligomerization).

The functionality of each HDS2 mutant was then assessed. To date, the only mutation within the HDS2 domain shown to impair function is the L1246R substitution in α-helix 5 that leads to vascular hemorrhaging and embryonic lethality (13). An additional report described the decreased viability of yeast cells containing Gea1p (the yeast ortholog of GBF1) with compound mutations in the HDS1 and the HDS2 domains, but it did not determine which mutation in which domain was responsible for the loss of viability (49, 50). We tested the functionality of each GBF1 variant by multiple, increasingly stringent readouts, including the ability to sustain Golgi architecture, recruit the COPI coat, sustain secretion, and impart viability to cells. We used a cellular replacement assay in which the endogenous GBF1 is inactivated with BFA, and the exogenously expressed BFA-resistant GBF1 constructs represent the only BFA-resistant GBF1 species in the cell.

We show that mutating the LMK1135 motif in α-helix 1 and the VLL1220 motif in α-helix 4 do not appear to significantly impact GBF1 function in any of the assays we used. This was somewhat surprising since the LMK1135 and the VLL1220 sequences are extremely highly conserved across the phylogenetic tree, and both triads reside within the middle of their respective α-helix. Perhaps this reflects flexibility of these helices and a higher threshold for tolerating substitutions.

In contrast, mutating the RDR1168 in α-helix 2 decreases GBF1 functionality to ~50% of wild-type GBF1 in supporting Golgi homeostasis (Fig. 2), COPI recruitment (Fig. 3), secretion (Fig. 4), and cell viability (Fig. 6). An even more severe inhibitory effect on GBF1 functions is caused by mutating the LF1266 in α-helix 6. The LF construct retains ~50% of the functionality of wild-type GBF1 in supporting Golgi homeostasis (Fig. 2) and COPI recruitment (Fig. 3) but is almost nonfunctional in secretion (Fig. 4) and cell viability (Fig. 6). The differential ability of LF to sustain some, but not all, functions of wild-type GBF1 suggests that HDS2 may participate in multiple activities, only some of which are compromised by the mutation. This raises the important point that multiple readouts of function might be needed to define whether a particular mutant form of an enzyme is functional. In our case, the ability of the LF construct to partially support Golgi homeostasis was not indicative of its inability to support the more stringent/demanding tests of secretion and viability. How can the LF construct function in Golgi homeostasis but be inactive in secretion or viability? The simplest explanation for our data is that the LF1266 motif participates in multiple interactions and that substituting the LF1266 residues with alanines affects those interactions differently. Although the LF1266AA mutation minimally affects the interactions required for sustaining Golgi homeostasis, it strongly compromises or perhaps completely abolishes the interactions required to sustain secretion and viability.

That a particular mutation within a protein may differently impact distinct functions of that protein is well known. For example, the WK228AA substitution in the Orc6 components of the origin recognition complex (ORC) that regulates both DNA replication and cytokinesis, preferentially inhibit cytokinesis but not DNA replication (3). Similarly, the T30N substitution in RF-like 2 (ARL2) inhibits mitochondrial functions of ARL2 without affecting its activity in regulating microtubule dynamics (45). In addition, mutating lysines 15 and 16 in ARF1 decrease its interaction with ASAP1 and AGAP1 significantly more than with Arf GAP1 (71), while mutating tyrosine 81 in ARF1 inhibits its interactions with AGAP1 while significantly promoting its ability to bind GGA (70). In most cases, the differences in functionality reflect differences in the ability of the mutant protein to interact with specific binding partners, and we propose that HDS2 participates in multiple interactions that show differential sensitivity to the LF mutation.

Why are the RDR and the LF mutants functionally compromised? Since GBF1 is active only while membrane associated, impaired membrane association could account for the lack of functionality. In agreement, mutations of RDR1168 and LF1266 decreased the efficiency of GBF1 targeting to the Golgi, with the RDR substitution having a more inhibitory effect than the LF substitution. The RDR substitutions changed charged amino acids, whereas the LF mutations aimed at disrupting the hydrophobic surface composed of W1, L4, F5, L7, and L8 within an amphipathic α-helix 6. The charged RDR residues appear more important than the hydrophobic LF-to-GBF1 association with Golgi membranes, suggesting an ionic component to membrane interaction.

The ~50% functionality of the RDR construct and its significantly reduced membrane association are consistent with a model in which the decreased cellular functionality is due to decreased membrane association rather than an impairment in activity. In contrast, a different scenario appears to unfold for the LF construct. Specifically, this mutant targets to the Golgi better than the RDR construct (Fig. 5); yet, it is almost completely inactive in sustaining secretion (Fig. 4) and cell viability (Fig. 6). This result is most consistent with a model in which the decreased cellular functionality of the LF construct is due to both reduced membrane association and an impairment in activity. Thus, our findings suggest that the RDR motif in α-helix 2 predominantly affects membrane targeting without significantly impacting other parameters of GBF1 activity, whereas the LF motif in α-helix 6 has a lower impact on Golgi targeting but inhibits downstream GBF1 activities.

The membrane-targeting function of α-helix 2 and α-helix 6 in HDS2 adds them to the NH_2-terminal domain of GBF1 and the HDS1 domain as novel structural motifs regulating membrane association of GBF1. This implies that targeting to the Golgi requires multiple, structurally separate regions of GBF1. The precise molecular mechanisms through which the RDR in α-helix 2 and the LF in α-helix 6 of the HDS2 domain regulate GBF1 membrane association and function remain to be defined by future work. It is possible that each or both motifs participate in intra-GBF1 interactions, but we think that unlikely, since all the HDS2 mutants showed normal overall structure when tested by Blue native gel electrophoresis (Fig. 2). Furthermore, no interaction between the HDS2 domain and the NH_2-terminal region of GBF1 or the HDS1 domain was detected by yeast two hybrid screens or in in vitro binding assays using recombinant fragments (51). Thus, it is more likely that the NH_2 terminus, the HDS1, and the α-helix 2 of

HDS2 may each directly and simultaneously bind to membrane components in a coincidence detection mechanism, in which multiple binding interactions regulate targeting efficiency.

The only known cellular proteins that bind to large fragments of GBF1 or the Gea2p yeast ortholog that contain the HDS2 domain (and additional domains) are the adipose triglyceride lipase (ATGL), involved in lipid droplet metabolism (21), and the Trs65 component of the TRAPPII complex, respectively (14). However, it is not known whether ATGL or Trs65 bind to the HDS2 domain within the tested fragments of GBF1 or Gea2p or to another region within the fragment. Furthermore, ATGL localizes to lipid droplets, but not the Golgi (11, 21), making it an unlikely candidate to mediate GBF1 association and function at the Golgi, while a GBF1-Trs65 interaction has not been as yet detected in mammalian cells.

Future work will be needed to dissect the exact molecular mechanism through which HDS2 may impact GBF1 function. It is possible that the HDS2 domain plays a direct allosteric role in the optimal positioning of the catalytic Sec7d of GBF1 on the membrane or has an indirect role in positioning the substrate ARF proximal to the Sec7d of GBF1 to optimize GDP/GTP exchange. Other models may be proposed, in which the HDS2 domain may interact with other traffic regulators, such as ARF GAPs, or with as yet unidentified proteins that facilitate secretory traffic.

The involvement of distinct structural motifs in regulating GBF1 functionality in cells might be indicative of a controlling mechanism to impart precise spatiotemporal restriction on GBF1-mediated ARF activation. It suggests a model in which the different domains may respond to and integrate multiple cellular signals to initiate ARF signaling cascades only at the correct place and time. Extensive enzymatic, structural, and mechanistic description of how each domain responds to cellular inputs and conveys molecular information to downstream effectors will be needed to understand the molecular network that regulates GBF1-mediated Golgi homeostasis, secretion and cell viability.

ACKNOWLEDGMENTS

The authors thank Drs. Rick Kahn, Paul Randazzo, and Melanie Styers for helpful comments.

GRANTS

This work was supported by a grant from the National Institutes of Health (National Institute of Allergy and Infectious Diseases R01 AI-125561) to G. A. Belov and E. Sztul, and from the National Science Foundation (MCB0744471) to E. Sztul. The content is solely the responsibility of the authors and does not necessarily represent the official views of the National Institutes of Health.

DISCLOSURES

No conflicts of interest, financial or otherwise, are declared by the authors.

AUTHOR CONTRIBUTIONS

G.A.B. and E.S. conceived and designed research; C.A.P., E.G.V., J.W., J.M.M., G.S., and E.L. performed experiments; C.A.P., E.G.V., J.M.M., and G.S. analyzed data; C.A.P. and E.G.V. interpreted results of experiments; C.A.P., E.G.V., and J.M.M. prepared figures; C.A.P., G.A.B., and E.S. drafted manuscript; C.A.P., G.A.B., and E.S. edited and revised manuscript; C.A.P., E.G.V., J.W., J.M.M., G.S., E.L., G.A.B., and E.S. approved final version of manuscript.

REFERENCES

1. **Alvarez C, Garcia-Mata R, Brandon E, Sztul E.** COPI recruitment is modulated by a Rab1b-dependent mechanism. *Mol Biol Cell* 14: 2116–2127, 2003. doi:10.1091/mbc.E02-09-0625.
2. **Armbruster K, Luschnig S.** The *Drosophila* Sec7 domain guanine nucleotide exchange factor protein Gartenzwerg localizes at the *cis*-Golgi and is essential for epithelial tube expansion. *J Cell Sci* 125: 1318–1328, 2012. doi:10.1242/jcs.096263.
3. **Balasov M, Huijbregts RP, Chesnokov I.** Functional analysis of an Orc6 mutant in *Drosophila*. *Proc Natl Acad Sci USA* 106: 10672–10677, 2009. doi:10.1073/pnas.0902670106.
4. **Balklava Z, Sztul E.** Studying membrane trafficking in the worm *C. elegans* by RNA interference. *Methods Cell Biol* 118: 51–68, 2013. doi:10.1016/B978-0-12-417164-0.00004-5.
5. **Belov GA, Feng Q, Nikovics K, Jackson CL, Ehrenfeld E.** A critical role of a cellular membrane traffic protein in poliovirus RNA replication. *PLoS Pathog* 4: e1000216, 2008. doi:10.1371/journal.ppat.1000216.
6. **Belov GA, Kovtunovych G, Jackson CL, Ehrenfeld E.** Poliovirus replication requires the N-terminus but not the catalytic Sec7 domain of ArfGEF GBF1. *Cell Microbiol* 12: 1463–1479, 2010. doi:10.1111/j.1462-5822.2010.01482.x.
7. **Béraud-Dufour S, Paris S, Chabre M, Antonny B.** Dual interaction of ADP ribosylation factor 1 with Sec7 domain and with lipid membranes during catalysis of guanine nucleotide exchange. *J Biol Chem* 274: 37629–37636, 1999. doi:10.1074/jbc.274.53.37629.
8. **Béraud-Dufour S, Robineau S, Chardin P, Paris S, Chabre M, Cherfils J, Antonny B.** A glutamic finger in the guanine nucleotide exchange factor ARNO displaces Mg^{2+} and the beta-phosphate to destabilize GDP on ARF1. *EMBO J* 17: 3651–3659, 1998. doi:10.1093/emboj/17.13.3651.
9. **Bhatt JM, Viktorova EG, Busby T, Wyrozumska P, Newman LE, Lin H, Lee E, Wright J, Belov GA, Kahn RA, Sztul E.** Oligomerization of the Sec7 domain Arf guanine nucleotide exch factor GBF1 is dispensable for Golgi localization and function but regulates degradation. *Am J Physiol Cell Physiol* 310: C456–C469, 2016. doi:10.1152/ajpcell.00185.2015.
10. **Boal F, Guetzoyan L, Sessions RB, Zeghouf M, Spooner RA, Lord JM, Cherfils J, Clarkson GJ, Roberts LM, Stephens DJ.** LG186: An inhibitor of GBF1 function that causes Golgi disassembly in human and canine cells. *Traffic* 11: 1537–1551, 2010. doi:10.1111/j.1600-0854.2010.01122.x.
11. **Bouvet S, Golinelli-Cohen MP, Contremoulins V, Jackson CL.** Targeting of the Arf-GEF GBF1 to lipid droplets and Golgi membranes. *J Cell Sci* 126: 4794–4805, 2013. doi:10.1242/jcs.134254.
12. **Bui QT, Golinelli-Cohen MP, Jackson CL.** Large Arf1 guanine nucleotide exchange factors: evolution, domain structure, and roles in membrane trafficking and human disease. *Mol Genet Genomics* 282: 329–350, 2009. doi:10.1007/s00438-009-0473-3.
13. **Chen J, Wu X, Yao L, Yan L, Zhang L, Qiu J, Liu X, Jia S, Meng A.** Impairment of cargo transportation caused by*gbf1* mutation disrupts vascular integrity and causes hemorrhage in zebrafish embryos. *J Biol Chem* 292: 2315–2327, 2017. doi:10.1074/jbc.M116.767608.
14. **Chen S, Cai H, Park SK, Menon S, Jackson CL, Ferro-Novick S.** Trs65p, a subunit of the Ypt1p GEF TRAPPII, interacts with the Arf1p exchange factor Gea2p to facilitate COPI-mediated vesicle traffic. *Mol Biol Cell* 22: 3634–3644, 2011. doi:10.1091/mbc.E11-03-0197.
15. **Cherfils J, Melançon P.** On the action of Brefeldin A on Sec7-stimulated membrane-recruitment and GDP/GTP exchange of Arf proteins. *Biochem Soc Trans* 33: 635–638, 2005. doi:10.1042/BST0330635.
16. **Cherfils J, Ménétrey J, Mathieu M, Le Bras G, Robineau S, Béraud-Dufour S, Antonny B, Chardin P.** Structure of the Sec7 domain of the Arf exchange factor ARNO. *Nature* 392: 101–105, 1998. doi:10.1038/32210.
17. **Citterio C, Vichi A, Pacheco-Rodriguez G, Aponte AM, Moss J, Vaughan M.** Unfolded protein response and cell death after depletion of brefeldin A-inhibited guanine nucleotide-exchange protein GBF1. *Proc Natl Acad Sci USA* 105: 2877–2882, 2008. doi:10.1073/pnas.0712224105.
18. **Claude A, Zhao BP, Kuziemsky CE, Dahan S, Berger SJ, Yan JP, Armold AD, Sullivan EM, Melançon P.** GBF1: A novel Golgi-associated BFA-resistant guanine nucleotide exchange factor that displays specificity for ADP-ribosylation factor 5. *J Cell Biol* 146: 71–84, 1999.
19. **Cole C, Barber JD, Barton GJ.** The Jpred 3 secondary structure prediction server. *Nucleic Acids Res* 36: W197–W201, 2008. doi:10.1093/nar/gkn238.

20. **Deng Y, Golinelli-Cohen MP, Smirnova E, Jackson CL.** A COPI coat subunit interacts directly with an early-Golgi localized Arf exchange factor. *EMBO Rep* 10: 58–64, 2009. doi:10.1038/embor.2008.221.
21. **Ellong EN, Soni KG, Bui QT, Sougrat R, Golinelli-Cohen MP, Jackson CL.** Interaction between the triglyceride lipase ATGL and the Arf1 activator GBF1. *PLoS One* 6: e21889, 2011. doi:10.1371/journal.pone.0021889.
22. **Faso C, Boulaflous A, Brandizzi F.** The plant Golgi apparatus: last 10 years of answered and open questions. *FEBS Lett* 583: 3752–3757, 2009. doi:10.1016/j.febslet.2009.09.046.
23. **García-Mata R, Szul T, Alvarez C, Sztul E.** ADP-ribosylation factor/COPI-dependent events at the endoplasmic reticulum-Golgi interface are regulated by the guanine nucleotide exchange factor GBF1. *Mol Biol Cell* 14: 2250–2261, 2003. doi:10.1091/mbc.E02-11-0730.
24. **Goujon M, McWilliam H, Li W, Valentin F, Squizzato S, Paern J, Lopez R.** A new bioinformatics analysis tools framework at EMBL-EBI. *Nucleic Acids Res* 38: W695–W699, 2010. doi:10.1093/nar/gkq313.
25. **Holloway ZG, Grabski R, Szul T, Styers ML, Coventry JA, Monaco AP, Sztul E.** Activation of ADP-ribosylation factor regulates biogenesis of the ATP7A-containing trans-Golgi network compartment and its Cu-induced trafficking. *Am J Physiol Cell Physiol* 293: C1753–C1767, 2007. doi:10.1152/ajpcell.00253.2007.
26. **Jones S, Jedd G, Kahn RA, Franzusoff A, Bartolini F, Segev N.** Genetic interactions in yeast between Ypt GTPases and Arf guanine nucleotide exchangers. *Genetics* 152: 1543–1556, 1999.
27. **Kahn RA.** Toward a model for Arf GTPases as regulators of traffic at the Golgi. *FEBS Lett* 583: 3872–3879, 2009. doi:10.1016/j.febslet.2009.10.066.
28. **Kawamoto K, Yoshida Y, Tamaki H, Torii S, Shinotsuka C, Yamashina S, Nakayama K.** GBF1, a guanine nucleotide exchange factor for ADP-ribosylation factors, is localized to the *cis*-Golgi and involved in membrane association of the COPI coat. *Traffic* 3: 483–495, 2002. doi:10.1034/j.1600-0854.2002.30705.x.
29. **Larkin MA, Blackshields G, Brown NP, Chenna R, McGettigan PA, McWilliam H, Valentin F, Wallace IM, Wilm A, Lopez R, Thompson JD, Gibson TJ, Higgins DG.** Clustal W and Clustal X version 2.0. *Bioinformatics* 23: 2947–2948, 2007. doi:10.1093/bioinformatics/btm404.
30. **Linstedt AD, Hauri HP.** Giantin, a novel conserved Golgi membrane protein containing a cytoplasmic domain of at least 350 kDa. *Mol Biol Cell* 4: 679–693, 1993. doi:10.1091/mbc.4.7.679.
31. **Lippincott-Schwartz J, Yuan LC, Bonifacino JS, Klausner RD.** Rapid redistribution of Golgi proteins into the ER in cells treated with brefeldin A: evidence for membrane cycling from Golgi to ER. *Cell* 56: 801–813, 1989. doi:10.1016/0092-8674(89)90685-5.
32. **Lowery J, Szul T, Seetharaman J, Jian X, Su M, Forouhar F, Xiao R, Acton TB, Montelione GT, Lin H, Wright JW, Lee E, Holloway ZG, Randazzo PA, Tong L, Sztul E.** Novel C-terminal motif within Sec7 domain of guanine nucleotide exchange factors regulates ADP-ribosylation factor (ARF) binding and activation. *J Biol Chem* 286: 36898–36906, 2011. doi:10.1074/jbc.M111.230631.
33. **Manolea F, Claude A, Chun J, Rosas J, Melançon P.** Distinct functions for Arf guanine nucleotide exchange factors at the Golgi complex: GBF1 and BIGs are required for assembly and maintenance of the Golgi stack and *trans*-Golgi network, respectively. *Mol Biol Cell* 19: 523–535, 2007. doi:10.1091/mbc.E07-04-0394.
34. **Mansour SJ, Skaug J, Zhao XH, Giordano J, Scherer SW, Melançon P.** p200 ARF-GEP1: a Golgi-localized guanine nucleotide exchange protein whose Sec7 domain is targeted by the drug brefeldin A. *Proc Natl Acad Sci USA* 96: 7968–7973, 1999. doi:10.1073/pnas.96.14.7968.
35. **Mazaki Y, Nishimura Y, Sabe H.** GBF1 bears a novel phosphatidylinositol-phosphate binding module, BP3K, to link PI3Kγ activity with Arf1 activation involved in GPCR-mediated neutrophil chemotaxis and superoxide production. *Mol Biol Cell* 23: 2457–2467, 2012. doi:10.1091/mbc.E12-01-0062.
36. **McNew JA, Sogaard M, Lampen NM, Machida S, Ye RR, Lacomis L, Tempst P, Rothman JE, Söllner TH.** Ykt6p, a prenylated SNARE essential for endoplasmic reticulum-Golgi transport. *J Biol Chem* 272: 17776–17783, 1997. doi:10.1074/jbc.272.28.17776.
37. **Meissner JM, Bhatt JM, Lee E, Styers ML, Ivanova AA, Kahn RA, Sztul E.** The ARF guanine nucleotide exchange factor GBF1 is targeted to Golgi membranes through a PIP-binding domain. *J Cell Sci* 131: jcs210245, 2018. doi:10.1242/jcs.210245.
38. **Monetta P, Slavin I, Romero N, Alvarez C.** Rab1b interacts with GBF1 and modulates both ARF1 dynamics and COPI association. *Mol Biol Cell* 18: 2400–2410, 2007. doi:10.1091/mbc.E06-11-1005. doi:10.1091/mbc.E06-11-1005.
39. **Monetta P, Slavin I, Romero N, Alvarez C.** Rab1b interacts with GBF1 and modulates both ARF1 dynamics and COPI association. *Mol Biol Cell* 18: 2400–2410, 2007. doi:10.1091/mbc.E06-11-1005.
40. **Mossessova E, Corpina RA, Goldberg J.** Crystal structure of ARF1*Sec7 complexed with Brefeldin A and its implications for the guanine nucleotide exchange mechanism. *Mol Cell* 12: 1403–1411, 2003. doi:10.1016/S1097-2765(03)00475-1.
41. **Mossessova E, Gulbis JM, Goldberg J.** Structure of the guanine nucleotide exchange factor Sec7 domain of human arno and analysis of the interaction with ARF GTPase. *Cell* 92: 415–423, 1998. doi:10.1016/S0092-8674(00)80933-2.
42. **Nakamura N, Rabouille C, Watson R, Nilsson T, Hui N, Slusarewicz P, Kreis TE, Warren G.** Characterization of a *cis*-Golgi matrix protein, GM130. *J Cell Biol* 131: 1715–1726, 1995. doi:10.1083/jcb.131.6.1715.
43. **Nawrotek A, Zeghouf M, Cherfils J.** Allosteric regulation of Arf GTPases and their GEFs at the membrane interface. *Small GTPases* 7: 283–296, 2016. doi:10.1080/21541248.2016.1215778.
44. **Nelson DS, Alvarez C, Gao YS, García-Mata R, Fialkowski E, Sztul E.** The membrane transport factor TAP/p115 cycles between the Golgi and earlier secretory compartments and contains distinct domains required for its localization and function. *J Cell Biol* 143: 319–331, 1998. doi:10.1083/jcb.143.2.319.
45. **Newman LE, Zhou CJ, Mudigonda S, Mattheyses AL, Paradies E, Marobbio CM, Kahn RA.** The ARL2 GTPase is required for mitochondrial morphology, motility, and maintenance of ATP levels. *PLoS One* 9: e99270, 2014. doi:10.1371/journal.pone.0099270.
46. **Niu TK, Pfeifer AC, Lippincott-Schwartz J, Jackson CL.** Dynamics of GBF1, a Brefeldin A-sensitive Arf1 exchange factor at the Golgi. *Mol Biol Cell* 16: 1213–1222, 2005. doi:10.1091/mbc.E04-07-0599.
47. **Opat AS, Houghton F, Gleeson PA.** Steady-state localization of a medial-Golgi glycosyltransferase involves transit through the *trans*-Golgi network. *Biochem J* 358: 33–40, 2001. doi:10.1042/bj3580033.
48. **Petris MJ, Mercer JF, Culvenor JG, Lockhart P, Gleeson PA, Camakaris J.** Ligand-regulated transport of the Menkes copper P-type ATPase efflux pump from the Golgi apparatus to the plasma membrane: a novel mechanism of regulated trafficking. *EMBO J* 15: 6084–6095, 1996.
49. **Peyroche A, Courbeyrette R, Rambourg A, Jackson CL.** The ARF exchange factors Gea1p and Gea2p regulate Golgi structure and function in yeast. *J Cell Sci* 114: 2241–2253, 2001.
50. **Peyroche A, Jackson CL.** Functional analysis of ADP-ribosylation factor (ARF) guanine nucleotide exchange factors Gea1p and Gea2p in yeast. *Methods Enzymol* 329: 290–300, 2001. doi:10.1016/S0076-6879(01)29090-9.
51. **Ramaen O, Joubert A, Simister P, Belgareh-Touzé N, Olivares-Sanchez MC, Zeeh JC, Chantalat S, Golinelli-Cohen MP, Jackson CL, Biou V, Cherfils J.** Interactions between conserved domains within homodimers in the BIG1, BIG2, and GBF1 Arf guanine nucleotide exchange factors. *J Biol Chem* 282: 28834–28842, 2007. doi:10.1074/jbc.M705525200.
52. **Randazzo PA, Terui T, Sturch S, Fales HM, Ferrige AG, Kahn RA.** The myristoylated amino terminus of ADP-ribosylation factor 1 is a phospholipid- and GTP-sensitive switch. *J Biol Chem* 270: 14809–14815, 1995. doi:10.1074/jbc.270.24.14809.
53. **Robin P, Rossignol B, Raymond MN.** Effect of microtubule network disturbance by nocodazole and docetaxel (Taxotere) on protein secretion in rat extraorbital lacrimal and parotid glands. *Eur J Cell Biol* 67: 227–237, 1995.
54. **Robineau S, Chabre M, Antonny B.** Binding site of brefeldin A at the interface between the small G protein ADP-ribosylation factor 1 (ARF1) and the nucleotide-exchange factor Sec7 domain. *Proc Natl Acad Sci USA* 97: 9913–9918, 2000. doi:10.1073/pnas.170290597.
55. **Rojo M, Emery G, Marjomäki V, McDowall AW, Parton RG, Gruenberg J.** The transmembrane protein p23 contributes to the organization of the Golgi apparatus. *J Cell Sci* 113: 1043–1057, 2000.
56. **Sáenz JB, Sun WJ, Chang JW, Li J, Bursulaya B, Gray NS, Haslam DB.** Golgicide A reveals essential roles for GBF1 in Golgi assembly and function. *Nat Chem Biol* 5: 157–165, 2009. doi:10.1038/nchembio.144.
57. **Saraste J, Svensson K.** Distribution of the intermediate elements operating in ER to Golgi transport. *J Cell Sci* 100: 415–430, 1991.
58. **Scheel J, Pepperkok R, Lowe M, Griffiths G, Kreis TE.** Dissociation of coatomer from membranes is required for brefeldin A-induced transfer of

Golgi enzymes to the endoplasmic reticulum. *J Cell Biol* 137: 319–333, 1997. doi:10.1083/jcb.137.2.319.

59. **Spang A, Herrmann JM, Hamamoto S, Schekman R.** The ADP ribosylation factor-nucleotide exchange factors Gea1p and Gea2p have overlapping, but not redundant functions in retrograde transport from the Golgi to the endoplasmic reticulum. *Mol Biol Cell* 12: 1035–1045, 2001. doi:10.1091/mbc.12.4.1035.
60. **Styers ML, O'Connor AK, Grabski R, Cormet-Boyaka E, Sztul E.** Depletion of β-COP reveals a role for COP-I in compartmentalization of secretory compartments and in biosynthetic transport of caveolin-1. *Am J Physiol Cell Physiol* 294: C1485–C1498, 2008. doi:10.1152/ajpcell.00010.2008.
62. **Szul T, Burgess J, Jeon M, Zinn K, Marques G, Brill JA, Sztul E.** The Garz Sec7 domain guanine nucleotide exchange factor for Arf regulates salivary gland development in *Drosophila*. *Cell Logist* 1: 69–76, 2011. doi:10.4161/cl.1.2.15512.
63. **Szul T, Garcia-Mata R, Brandon E, Shestopal S, Alvarez C, Sztul E.** Dissection of membrane dynamics of the ARF-guanine nucleotide exchange factor GBF1. *Traffic* 6: 374–385, 2005. doi:10.1111/j.1600-0854.2005.00282.x.
64. **Szul T, Grabski R, Lyons S, Morohashi Y, Shestopal S, Lowe M, Sztul E.** Dissecting the role of the ARF guanine nucleotide exchange factor GBF1 in Golgi biogenesis and protein trafficking. *J Cell Sci* 120: 3929–3940, 2007. doi:10.1242/jcs.010769.
65. **Tannous BA, Kim DE, Fernandez JL, Weissleder R, Breakefield XO.** Codon-optimized Gaussia luciferase cDNA for mammalian gene expression in culture and in vivo. *Mol Ther* 11: 435–443, 2005. doi:10.1016/j.ymthe.2004.10.016.
66. **Van De Moortele S, Picart R, Tixier-Vidal A, Tougard C.** Nocodazole and taxol affect subcellular compartments but not secretory activity of GH3B6 prolactin cells. *Eur J Cell Biol* 60: 217–227, 1993.
67. **Wang S, Meyer H, Ochoa-Espinosa A, Buchwald U, Onel S, Altenhein B, Heinisch JJ, Affolter M, Paululat A.** GBF1 (Gartenzwerg)-dependent secretion is required for *Drosophila* tubulogenesis. *J Cell Sci* 125: 461–472, 2012. doi:10.1242/jcs.092551.
68. **Wright J, Kahn RA, Sztul E.** Regulating the large Sec7 ARF guanine nucleotide exchange factors: the when, where and how of activation. *Cell Mol Life Sci* 71: 3419–3438, 2014. doi:10.1007/s00018-014-1602-7.
69. **Xu Y, Martin S, James DE, Hong W.** GS15 forms a SNARE complex with syntaxin 5, GS28, and Ykt6 and is implicated in traffic in the early cisternae of the Golgi apparatus. *Mol Biol Cell* 13: 3493–3507, 2002. doi:10.1091/mbc.E02-01-0004.
70. **Yoon HY, Bonifacino JS, Randazzo PA.** In vitro assays of Arf1 interaction with GGA proteins. *Methods Enzymol* 404: 316–332, 2005. doi:10.1016/S0076-6879(05)04028-0.
71. **Yoon HY, Jacques K, Nealon B, Stauffer S, Premont RT, Randazzo PA.** Differences between AGAP1, ASAP1 and Arf GAP1 in substrate recognition: interaction with the N-terminus of Arf1. *Cell Signal* 16: 1033–1044, 2004. doi:10.1016/S0898-6568(04)00026-9.
72. **Zhao X, Claude A, Chun J, Shields DJ, Presley JF, Melançon P.** GBF1, a *cis*-Golgi and VTCs-localized ARF-GEF, is implicated in ER-to-Golgi protein traffic. *J Cell Sci* 119: 3743–3753, 2006. doi:10.1242/jcs.03173.
73. **Zhao X, Lasell TK, Melançon P.** Localization of large ADP-ribosylation factor-guanine nucleotide exchange factors to different Golgi compartments: evidence for distinct functions in protein traffic. *Mol Biol Cell* 13: 119–133, 2002. doi:10.1091/mbc.01-08-0420.